Journal of Southeast University (English Edition) Vol. 21, No. 3, pp. 324 – 329 Sept. 2005 ISSN 1003—7985

Classification of forearm action surface EMG signals based on fractal dimension

Hu Xiao Wang Zhizhong Ren Xiaomei

(Department of Biomedical Engineering, Shanghai Jiaotong University, Shanghai 200030, China)

Abstract: Surface electromyogram (EMG) signals were identified by fractal dimension. Two patterns of surface EMG signals were acquired from 30 healthy volunteers' right forearm flexor respectively in the process of forearm supination (FS) and forearm pronation (FP). After the raw action surface EMG (ASEMG) signal was decomposed into several sub-signals with wavelet packet transform (WPT), five fractal dimensions were respectively calculated from the raw signal and four sub-signals by the method based on fuzzy self-similarity. The results show that calculated from the sub-signal in the band 0 to 125 Hz, the fractal dimensions of FS ASEMG signals and FP ASEMG signals distributed in two different regions, and its error rate based on Bayes decision was no more than 2.26%. Therefore, the fractal dimension is an appropriate feature by which an FS ASEMG signal is distinguished from an FP ASEMG signal.

Key words: action surface electromyogram (ASEMG) signal; fractal dimension; wavelet packet transform (WPT); fuzzy self-similarity; Bayes decision

A surface electromyogram (EMG) signal recorded from the skin surface over limb muscles in the process of limb actions is called an action surface electromyogram (ASEMG) signal. Because ASEMG signals contain the electrical and functional properties of limb muscle contraction, some features extracted from ASEMG signals can be used to identify different patterns of ASEMG signals and control limb prostheses[1-3]. So far, many parameters have been applied to represent the features. In the control system which Hudgins et al.[1] devised for powered upper-limb prosthesis, they utilized some time-domain parameters such as zero crossings of the ASEMG signal. Because of the random nature of the raw ASEMG signal, the ASEMG signal was also analyzed as a stochastic process. For example, Chang et al.[2] used the cepstral coefficients of the ASEMG signal as the control command of the man-machine interface. Later, some time-frequency features of the ASEMG signal[3] were used to describe the characteristics of the ASEMG signal.

However, the ASEMG signal is very complex and nonlinear[4], so there is still much work to do so as to make a right decision for different ASEMG signal patterns. In recent years, nonlinear dynamics has been greatly developed[5,6] and it has been clear that simple nonlinear systems can exhibit highly complex behavior. In a complex signal exists the self-similarity phenomenon, that is, there is a smaller structure that resembles the larger scale structure in such complex medical signals as EMG, EEG and ECG signals[7]. Fractal dimension can be applied to determine the self-similarity and has been applied in the case of the surface EMG signal[8].

However, there are two factors that affect the calculation of the fractal dimension from surface EMG signals. One is that the measured value of fractal dimension calculated by the GP algorithm[9] is very sensitive to the signal's initial value or the initial position of the hypersphere[6]. In order to reduce the sensitivity, Sarkar and Leong[6] proposed the method based on a fuzzy self-similarity to calculate the fractal dimension. The other is that an ASEMG signal is a signal with low signal to noise ratio[10]. In this paper, we categorize information into two kinds: discriminable information and noise. The former includes the features by which one pattern of ASEMG signal can be accurately distinguished from another pattern. Some information in an ASEMG signal is able to characterize some common characteristics of the ASEMG signal but is not helpful for identifying different patterns of the ASEMG signal, so the information is categorized as noise. In order to evaluate fractal dimension by which different patterns of ASEMG signals are accurately identified, an important step is to effectively reduce noise from the ASEMG signal before fractal dimension is estimated.

Hence, every ASEMG signal was decomposed into several sub-signals with WPT in this paper. Then the

Received 2005-03-22.

Foundation items: The National Natural Science Foundation of China (No. 60171006), the National Basic Research Program of China (973 Program) (No. 2005CB724303).

Biographies: Hu Xiao (1969—), male, PhD; Wang Zhizhong (corresponding author), male, PhD, professor, zzwang@sjtu.edu.cn.

authors calculated fractal dimensions from its raw signal and its sub-signals and compared their contribution to identifying ASEMG signals. Finally a useful frequency band was determined.

1 Material and Methodology

1.1 ASEMG acquisition

All ASEMG signals were recorded from the right forearm flexor of 30 healthy volunteers in the EMG room at Huashan Hospital in Shanghai, China. Two 5 mm diameter electrodes, set 2 cm apart, were put on the skin surface over the flexor carpi radialis on the right forearm along the flexor. The negative electrode was placed nearer every volunteer's heart than the positive electrode to form a differential comparator amplifier. The sampling frequency was 1 000 Hz. During the acquisition process, every volunteer was instructed to complete two different kinds of limb actions: FS and FP. Two patterns of ASEMG signals lasting more than 1 000 ms^{-1} were recorded elaborately from every volunteer's forearm flexor: one during FS and the other during FP. Thus, among the 60 sets of ASEMG signals acquired, there were two ASEMG signal patterns: FS ASEMG signal and FP ASEMG signal, 30 sets for each pattern.

1.2 Wavelet packet transform

Given a finite energy signal whose scaling space is assumed as U_0^0, WPT can decompose U_0^0 into small subspaces U_j^n in a dichotomous way[11]. See Fig. 1. U_j^{n-1} shows the n-th subspace on the j-th resolution level.

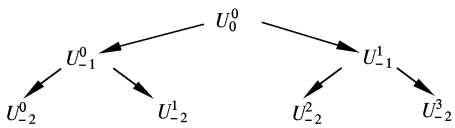

Fig. 1 Tree structure of WPT

The dichotomous way is realized by the following recursive scheme:

$$U_{j+1}^n = U_j^{2n} \oplus U_j^{2n+1} \qquad j \in \mathbf{Z};\ n \in \mathbf{Z}^+ \tag{1}$$

where $j(j \leqslant 0)$ is the resolution level; $\oplus$ denotes direct sum; U_{j+1}^n, U_j^{2n} and U_j^{2n+1} are three close spaces corresponding to $u_n(t)$, $u_{2n}(t)$ and $u_{2n+1}(t)$. $u_n(t)$ satisfies the following equation[11]:

$$\left.\begin{aligned} u_{2n}(t) &= \sqrt{2}\sum_{k\in\mathbf{Z}} h(k)\,u_n(2t-k) \\ u_{2n+1}(t) &= \sqrt{2}\sum_{k\in\mathbf{Z}} g(k)\,u_n(2t-k) \end{aligned}\right\} \tag{2}$$

where the function $u_0(t)$ can be identified with the scaling function φ and $u_1(t)$ with the mother wavelet ψ; $h(k)$ and $g(k)$ are the coefficients of a low-pass and a high-pass filter, respectively; the sequence of function $\{u_n\}(n = 0, 1, \ldots, \infty)$, which is generated from a given function u_0 by Eq. (2), is called the wavelet packet basis function.

When $s(t)$ is decomposed to the second resolution level ($j = -2$) with WPT, the whole scaling space U_0^0 with frequencies in the interval $(0, 2^{-1}f_s]$ is divided into four subspaces with frequencies correspondingly in the interval $((n-1)2^{j-1}f_s, n2^{j-1}f_s]$, $n = 1, 2, 3, 4$. The sub-signal at U_j^{n-1}, the n-th subspace on the j-th level, can be reconstructed by

$$s_j^n(t) = \sum_k D_k^{j,n}\,\psi_{j,k}(t) \qquad k \in \mathbf{Z} \tag{3}$$

where $D_k^{j,n}$ is the wavelet packet coefficients at U_j^{n-1}, and $\psi_{j,k}(t)$ is the wavelet function.

1.3 Fractal dimension

The most common way to calculate fractal dimension is correlation dimension (denoted by D_2). Correlation dimension determines how the distribution of a signal set scales up/down with decreasing/increasing radius of each hypersphere. The correlation dimension is often obtained by using the GP algorithm[9]. In the algorithm, correlation integral function is applied as follows:

$$I_c(r) = \frac{1}{N(N-1)}\sum_{i=1}^{N}\sum_{j=1,j\neq i}^{N}\theta(d_{ij}, r) \tag{4}$$

where

$$\theta(d_{ij}, r) = \begin{cases} 1 & \text{if } d_{ij} \leqslant r \\ 0 & \text{if } d_{ij} > r \end{cases} \qquad i \neq j \tag{5}$$

is Heaviside unit function, r is the radius of the hypersphere, and d_{ij} is an Euclidean distance between point y_i and y_j in the reconstruction phase space (details in appendix A).

D_2 can be estimated using the following formula:

$$D_2 = \lim_{r\to 0}\frac{\log(I_c(r))}{\log(r)} \tag{6}$$

However, D_2 calculated by the traditional GP algorithm varies significantly with slight change in point position or with slight change of the initial hypersphere position. It happens because the signal points inside the hypersphere are treated equally and the signal points just outside the hypersphere are not considered due to Heaviside unit function $\theta(d_{ij}, r)$. To reduce the effect, Sarkar and Leong[6] replaced $\theta(d_{ij}, r)$ with the Guassian function

$$u(d_{ij}, r) = \exp\left(-\frac{d_{ij}^2}{r^2}\right) \qquad i \neq j \tag{7}$$

Here, because the boundary of the hypersphere is not sharp but fuzzy, the plot of $\log(I_c(r))$ *vs.* $\log(r)$ becomes smooth. The correlation dimension varies less with the change of initial position so that it can be measured more accurately[6]. In this paper, we employ the method based on the fuzzy self-similarity to evalu-

ate fractal dimension of an ASEMG signal.

2 Results

2.1 Choice of embedding dimension *m*

In the GP algorithm, D_2 is obtained by the $D_2(m)$ slope, $m = 1, 2, 3, \ldots$. When $D_2(m)$ does not change with m increasing, this $D_2(m_0)$ is regarded as the estimate value of D_2 (see Fig. 2). Fig. 2 is the D_2-m of an FS ASEMG signal and an FP ASEMG signal from the same volunteer. From Fig. 2, we find that $D_2(m)$ can trend to a stable value when $m > 17$. After analyzing statistically D_2-m of all analyzed signals, we found that when $m > 15$, $D_2(m)$ can trend to a stable value, no matter whether the analyzed signal is a raw signal or a sub-signal.

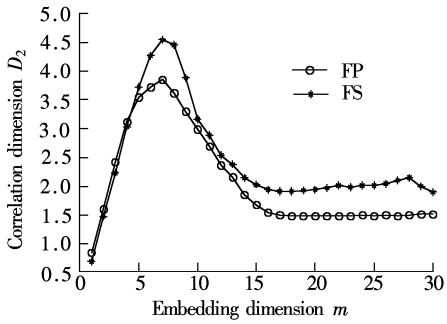

Fig. 2 Correlation dimension vs. embedding dimension

2.2 Choosing *r* range for ASEMG signal with finite sampling points

r is the radius of the hypersphere. An appropriate r must be chosen so that D_2 can describe the structure of self-similarity in the EMG signal. Choosing an appropriate r range for the Heaviside function is a worrisome business requiring much computation time. For signals with infinite sampling points, r should be set $r \to 0$. But for real signals, the finite sampling points force us to calculate the fractal dimension at a larger r. In this paper, we get the r range by observing the results of the following experiment. From half the minimum of the distances between any two points in reconstruction space to the maximum of the distances, the range is divided into 99 equal intervals with 100 points. The value at the points is regarded as r. The points from small to large are identified by the number k from 1 to 100. According to Eq. (6), for all the identical pattern signals, $\log(I_c(r))$ is plotted against $\log(r)$ in the same plot. Fig. 3 shows $\log(I_c(r))$ vs. $\log(r)$ for the sub-signal in U^0_{-2}. According to Buczkowski's study[12], it is noticeable from Fig. 3 that there are several dimensions for every signal no matter whether it is an FP or FS signal in U^0_{-2}. The values at the middle flatter curve of $\log(I_c(r))$ vs. $\log(r)$ are chosen as r, so the points are about from 10 to 20 for an FP or FS signal in U^0_{-2}. With the same method, we get r range for the sub-signals in U^0_0, U^0_{-1}, U^1_{-1} and U^1_{-2}. Their k is listed in Tab. 1.

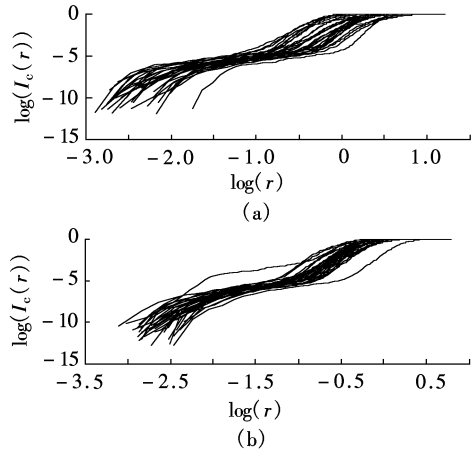

Fig. 3 Plot of $\log(I_c(r))$ vs. $\log(r)$ to determine an appropriate r. (a) For filtered FP signals; (b) For filtered FS signals

Tab. 1 The range of k

Subspace	U^0_0	U^0_{-1}	U^1_{-1}	U^0_{-2}	U^1_{-2}
k	10 to 20	5 to 15	40 to 50	10 to 20	20 to 30

2.3 Distribution of fractal dimensions

For every FP and FS signal, the dimension of its raw signal in U^0_0 and the dimensions of its sub-signals in U^0_{-1}, U^1_{-1}, U^0_{-2} and U^1_{-2} were calculated, and the fractal dimensions were respectively represented with D_{00}, D_{01}, D_{11}, D_{02} and D_{12}. Fig. 4 shows the distribution of the fractal dimensions of 30 sets of FP signals and 30 sets of FS signals. From Fig. 4, we obtained two results. One was that the fractal dimensions of raw signals were more widely dispersed than the fractal dimensions of sub-signals. D_{00} ranged from 0.5 to 3, no matter whether D_{00} was of FS signal or of FP signal. However, the fractal dimensions of sub-signals concentrated on a narrower range. The range became much smaller if D_{01} and D_{02} of the FP sub-signal or of the FS sub-signal was considered alone (see Tab. 2). The other was that the FS signal seemed to be distinguished from the FP signal by D_{01} or D_{02}, not by the other fractal dimensions. As for D_{00}, D_{11} and D_{12}, the fractal dimensions of FS signals were mixed completely together with those of FP signals. However, for D_{01} and D_{02}, the fractal dimensions of most FS signals and of most FP signals respectively distributed in two separable regions, and the fractal dimensions of most FS signals were larger than those of most FP signals. Specially, D_{02} region of the FS signal did not superpose with that of the FP signal, and all FS ASEMG signals could be completely distinguished from all FP ASEMG signals by their D_{02}. Some statistical parameters on D_{01} and D_{02} were listed in Tab. 2.

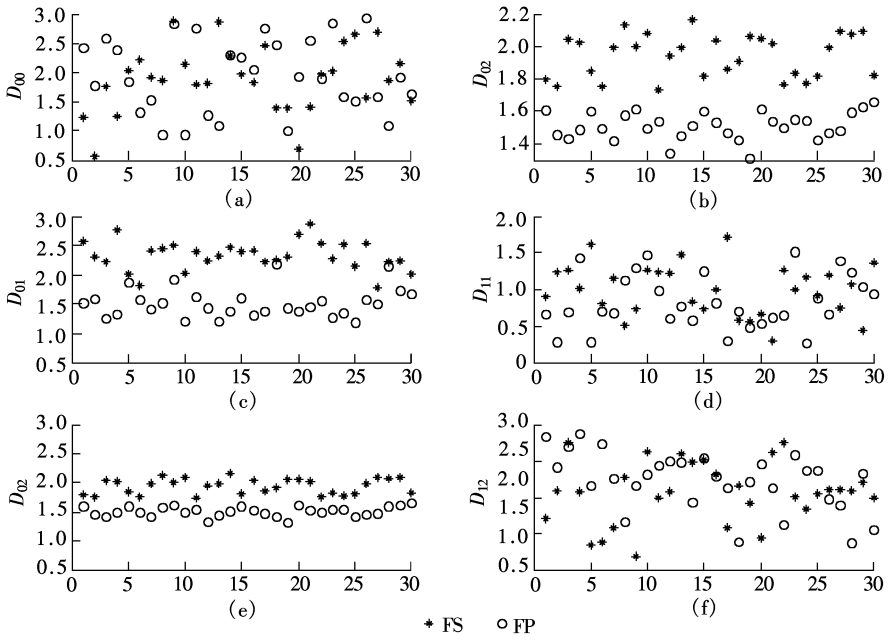

Fig. 4 Distribution of fractal dimensions

Tab. 2 Statistical parameters on D_{01} and D_{02}

Parameters	D_{01}		D_{02}	
	FP	FS	FP	FS
Minimum value	1.193 3	1.781 2	1.312 2	1.737 2
Maximum value	2.184 9	2.866 4	1.655 4	2.166 1
Average value μ	1.521 7	2.331 8	1.511 6	1.944 1
Standard deviation σ	0.254 1	0.252 4	0.085 0	0.132 2
Error decision rate R_e/%	5.49		2.26	

2.4 Error decision rate based on Bayes decision

Let ω_1 and ω_2 be the two classes (FS and FP ASEMG signal patterns) to which our patterns belong. Feature vector $\boldsymbol{x}$ represents an unknown pattern. The Bayes rule is

$$P(\omega_i/\boldsymbol{x}) = \frac{p(\boldsymbol{x}/\omega_i)P(\omega_i)}{\sum_{i=1}^{2} p(\boldsymbol{x}/\omega_i)P(\omega_i)} \tag{8}$$

where $p(\omega_i/\boldsymbol{x})$ is the i-th conditional probability and $P(\omega_i)$ is priori probability. In this paper, $P(\omega_1) = P(\omega_2) = 1/2$. $p(\boldsymbol{x}/\omega_i)$ is the class-conditional probability density function. One of the most commonly encountered probability density functions in practice is the Gaussian or normal density function. The major reasons for its popularity are its computational tractability and the fact that it models adequately a large number of cases. According to the results above, D_{01} and D_{02} can be regarded as the feature by which two patterns of ASEMG signals are identified. The normal density functions of feature space constituted by 30 D_{01} or 30 D_{02} are depicted in Fig. 5. The normal distribution parameters μ and σ are listed in Tab. 2. The result that σ of D_{02} is much less than σ of D_{01} means that D_{02} can describe more accurately nonlinear properties of ASEMG signals than σ of D_{01}.

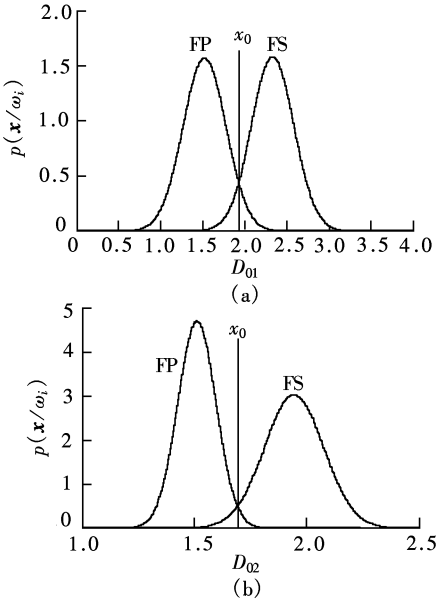

Fig. 5 Normal distribution fitting curves of the feature space constituted by D_{01} or D_{02}. (a) D_{01}; (b) D_{02}

The Bayes classification rules can be stated as

If $p(\omega_1/\boldsymbol{x}) > p(\omega_2/\boldsymbol{x})$, $\boldsymbol{x}$ is classified to ω_1

If $p(\omega_1/\boldsymbol{x}) < p(\omega_2/\boldsymbol{x})$, $\boldsymbol{x}$ is classified to ω_2

If the straight line at x_0 is the threshold partitioning the feature space into regions: FP and FS (see Fig. 5), all values of $\boldsymbol{x}$ in FP are classified as ω_1, and all values of $\boldsymbol{x}$ in FS are classified as ω_2. It is obvious that decision errors are unavoidable. The total probability, P_e, of committing a decision error is given by

$$P_e = \frac{1}{2}\int_{-\infty}^{x_0} p(\boldsymbol{x}/\omega_2)\,\mathrm{d}\boldsymbol{x} + \frac{1}{2}\int_{x_0}^{\infty} p(\boldsymbol{x}/\omega_1)\,\mathrm{d}\boldsymbol{x} \tag{9}$$

The error decision rate is calculated by

$$R_e = P_e \times 100\% \quad (10)$$

x_0 is the D_{01} or D_{02} value at the cross point of the normal density functions. For D_{01} and D_{02}, x_0 respectively are 1.927 6 and 1.692 2. In other words, if $D_{01} >$ 1.927 6, ASEMG signal is classified as FS pattern; otherwise, as FP pattern. In the same way, if $D_{02} >$ 1.692 2, ASEMG signal is classified as FS pattern; otherwise, as FP pattern. The error decision rates of D_{01} and D_{02} are respectively 5.49% and 2.26%.

3 Discussion

In the forearm flexor, there are many muscles (e.g. brachioradialis, pronator teres, flexor carpi radialis, flexor digitorum superficialis, etc.) taking charge of or assisting forearm actions. Major motor unit action potentials (MUAPs) of ASEMG signals analyzed in this study obviously come from the muscles. When a volunteer wants to take FS or FP, the motor units (MUs) of the muscles responsible for the limb action are stimulated by excitation from the ulnar or median nerve to actively change the muscles contraction level, so MUAPs from the muscles increase and most MUAPs from other muscles do not increase. Because the tissues between MUs and the surface electrodes have the effect of a low pass filter on MUAPs[10], MUAPs from the MUs closer to surface electrode have stronger amplitude and higher frequency, and MUAPs from the farther or deeper MUs have weaker amplitude and lower frequency. MUAP is the basis unit of the ASEMG signal. The properties (such as spectral energy distribution) of the ASEMG signal therefore change with the change of the different muscles' contribution levels. It is clear that between forearm action and its ASEMG signal there is a relationship which can be signified with some physical parameters such as amplitude, frequency or fractal dimension. Therefore, the parameters extracted from the local frequency band should more accurately generalize the general characteristics of FS ASEMG signal pattern and FP ASEMG signal pattern than the parameters from the whole frequency band.

In order to remove the noise, Xu and Xiao[10] designed a digital filter with a weighted window. Although the digital filter has good performance, the performance of the filter depends on the properties of surface EMG signal and an appropriately weighted window. The ASEMG signal is obviously a non-stationary signal, so an appropriately weighted window should be dependent on time. Thus, designing the appropriately weighted window will become more difficult and consume more time. Because of the adaptive time-frequency window of WPT, the components in the surface EMG signal can be distributed in their own frequency bands by WPT. On the other hand, different frequency resolutions for different regions in the frequency spectra are easily selected. WPT can therefore act as a filter with which the discriminable information is separated from the noise.

When fractal dimension is calculated directly from the raw ASEMG signal, the fractal dimension cannot undoubtedly be used as the feature which identifies FS ASEMG signal and FP ASEMG signal, because D_{00} of two patterns of ASEMG signals mix together. Obviously, it is the noise in the 250 to 500 Hz band that interferes with the accurate calculation of fractal dimension. However, fractal dimensions calculated from the sub-signals in U^0_{-1} (0 to 250 Hz) and U^0_{-2} (0 to 125 Hz) can take on general characteristics of different patterns of ASEMG signals, because D_{01} or D_{02} of most FS ASEMG signals are bigger than those of most FP ASEMG signals. Even FP and FS ASEMG signals can be completely identified by their D_{02}. FS ASEMG signals cannot be separated from FP signals by D_{11} and D_{12}, because D_{11} and D_{12} of FS ASEMG signals mix together with those of FP ASEMG signals. So we could infer that the noise energy in 125 to 500 Hz is much more than the discriminable information energy. Note that the noise may include the information which reflects the common information about the surface EMG signal but does not reflect the general characteristics about FP ASEMG signal pattern or FS ASEMG signal pattern. The results show that ASEMG signals in 0 to 125 Hz should hide most of the discriminable information.

In summary, the results demonstrated that fractal dimension could be used to determine the functional characteristics of limb muscles like the time domain parameters, cepstral coefficients and the time-frequency features. When noise in the raw ASEMG signal is reduced much, the fractal dimension of the ASEMG signal could accurately describe the nonlinear properties of different ASEMG signals.

4 Conclusion

The fuzzy similarity-based correlation dimension is an efficient method to calculate the fractal dimension from a complex ASEMG signal. The fractal dimension calculated by the method can describe the nonlinear properties of ASEMG signals. The fractal dimension estimated from ASEMG signals in 0 to 125 Hz is able to accurately identify FS ASEMG signals and FP ASEMG signals.

Appendix A *m*-dimensional phase space reconstruction

According to Takens' theorem, in order to suffi-

ciently disclose the information being hided medical time series, a time series, x_i, $i = 1, 2, \ldots, L$, is often turned into a new m-dimensional phase space in the following way. L is the length of the signal.

$$y_1 = \{x_1, x_{1+\tau}, \ldots, x_{1+(m-1)\tau}\}$$
$$y_2 = \{x_2, x_{2+\tau}, \ldots, x_{2+(m-1)\tau}\}$$
$$\vdots$$
$$y_i = \{x_i, x_{i+\tau}, \ldots, x_{i+(m-1)\tau}\}$$
$$\vdots$$
$$y_N = \{x_N, x_{N+\tau}, \ldots, x_{N+(m-1)\tau}\}$$

where N is the number of the points in the phase space ($N = L - (m-1)\tau$). In the reconstruction phase space, there are two important parameters: embedding dimension m and time delay τ. Because real ASEMG signal is finite and noisy, an appropriate τ must be chosen to ensure that the elements of y_i are independent and that the same τ can be used for all embedding dimensions m. Many methods have been developed to gain an appropriate τ, they include the autocorrelation function, the mutual information and C-C method[5]. Due to its convenience and fast calculation, in this paper the autocorrelation function is adopted to get the time delay τ which is determined by the first zero of the autocorrelation function. An embedding dimension m should satisfy the condition[13] $m \geqslant 2D + 1$ where D is the fractal dimension of the real medical signal.

References

[1] Hudgins B, Parker P, Scott R N. A new strategy for multifunction myoelectric control [J]. *IEEE Trans Biomed Eng*, 1993, **40**(1): 82 − 94.

[2] Chang G C, Kang W J, Luh J J, et al. Real-time implementation of electromyogram pattern recognition as a control command of man-machine interface [J]. *Med Eng Phys*, 1996, **18**(7): 529 − 537.

[3] Englehart K, Hudgins B, Parker P A, et al. Classification of the myoelectric signal using time-frequency based representations [J]. *Med Eng Phy*, 1999, **21**(6): 431 − 438.

[4] Lei M, Wang Z Z, Feng Z J. Detecting nonlinearity of action surface EMG signal [J]. *Physics Letters A*, 2001, **290**(6): 297 − 303.

[5] Kim H S, Eykholt R, Salas J D. Nonlinear dynamics, delay times, and embedding windows [J]. *Physica D*, 1999, **127**(1): 48 − 60.

[6] Sarkar M, Leong T Y. Characterization of medical time series using fuzzy similarity-based fractal dimensions [J]. *Artificial Intelligence in Medicine*, 2003, **27**(2): 201 − 222.

[7] Eke A, Herman P, Kocsis L, et al. Fractal characterization of complexity in temporal physiological signals [J]. *Physiol Meas*, 2002, **23**(1): 1 − 38.

[8] Gupta V, Suryanarayanan S, Reddy N P. Fractal analysis of surface EMG signals from the biceps [J]. *International Journal of Medical Informatics*, 1997, **45**(3): 185 − 192.

[9] Grassberger P, Procaccia I. Measuring the strangeness of strange attractors [J]. *Physica D*, 1983, **9**(2): 189 − 208.

[10] Xu Z Q, Xiao S J. Digital filter design for peak detection of surface EMG [J]. *Journal of Electromyography and Kinesiology*, 2000, **10**(4): 275 − 281.

[11] Coifman R R, Wickerhauser M V. Entropy-based algorithms for best basis selection [J]. *IEEE Trans Inform Theom*, 1992, **38**(2): 713 − 718.

[12] Buczkowski S, Hildgen P, Cartilier L. Measurements of fractal dimension by box-counting: a critical analysis of data scatter [J]. *Physica A*, 1998, **252**(1): 23 − 34.

[13] Parker T S, Chua L O. *Practical numerical algorithms for chaotic systems* [M]. New York: Springer-Verlag, 1989. 193 − 194.

基于分形维前臂动作表面肌电信号的分类

胡　晓　王志中　任小梅

(上海交通大学生物医学工程系, 上海 200030)

摘要: 通过分形维对表面肌电信号进行识别分类. 在 30 个健康志愿者做前臂内旋和外旋时,从他们的右前臂肌前群分别采集 2 类动作表面肌电信号. 当原始动作表面肌电信号用小波包变换分解成几个子信号后,采用一种基于模糊自相似性的方法计算原始信号和 4 个子信号的分形维. 结果表明:从频带 0 ~ 125 Hz 的子信号求得的内旋和外旋动作表面肌电信号的分形维有各自的范围;通过该分形维进行 Bayes 决策时,错误识别率仅 2.26%. 因此,该分形维适合用来识别内旋和外旋动作表面肌电信号.

关键词: 动作表面肌电信号;分形维;小波包变换;模糊自相似性;Bayes 决策

中图分类号: R318.04